Geofísica Internacional (2003), Vol. 42, Num. 1, pp. 101-114

Frontal subduction of a cool surface water mass in the Gulf of Tehuantepec, Mexico

A. Trasviña[1], E. D. Barton[2], H. S. Vélez[3] and J. Brown[4]
[1] *CICESE, La Paz BCS, Mexico*
[2] *University of Wales, Menai Bridge, United Kingdom*
[3] *Universidad Autónoma Metropolitana, Iztapalapa, México, D.F., México*
[4] *Fisheries Laboratories, Suffolk, United Kingdom*

Received: September 5, 2001; accepted: February 25, 2002

RESUMEN

Los eventos de viento del norte en el Golfo de Tehuantepec generan grandes giros cálidos e intensos chorros de corriente hacia afuera de la costa. Estos últimos producen abordaje de aguas subsuperficiales y forman 'parches' de agua superficial fría (densa). En la frontera entre giros y parches se generan frentes intensos de densidad. Una fracción importante del agua fría se hunde bajo estos giros. El fenómeno se observa como lentes (giros) dentro de la picnoclina del giro cálido principal, son estables e interactúan con éste. Se presenta evidencia observacional de la existencia de dos de estas lentes. La presencia de subducción se confirma mediante argumentos cualitativos (observaciones del flujo y del campo de densidad) y mediante argumentos de vorticidad. La tasa de subducción puede alcanzar los 80 m d^{-1}. Se presente un esquema conceptual revisado del proceso de generación de giros: a) durante un evento la corriente hacia fuera de la costa produce abordaje del agua subsuperficial y establece el gradiente inicial de densidad; b) también durante el evento, el gradiente horizontal de densidad se mantiene por advección lateral de agua cálida; c) después del evento se separa un chorro costero cálido de la costa occidental del golfo, alcanza el golfo central y adquiere rotación anticiclónica; d) la subducción inicia por procesos intensos de convergencia donde el chorro cálido choca con el agua fría; e) el giro 'maduro' se propaga hacia afuera de la costa acarreando un lente de subducción en su frontera.

PALABRAS CLAVE: Golfo de Tehuantepec, dinámica de giros, subducción, frentes, abordaje.

ABSTRACT

The southward wind events in the Gulf of Tehuantepec generate large warm eddies and strong offshore current jets that produce entrainment of subsurface waters into the upper ocean resulting in cool (dense) water masses. Strong frontal features occur at the boundary between warm eddies and cool patches. An important fraction of the cool water is subducted beneath these eddies as intrapycnocline 'lenses' (eddies) within the boundary of a larger eddy. These small eddies are stable and interact with the larger one. Observational evidence of two such lenses is presented. Qualitative arguments based on observed flow and density fields, as well as vorticity arguments, confirm the existence of subduction processes. The magnitude of the subduction rate is estimated as large as 80 m d^{-1}. A revised conceptual scheme of the eddy generating process is summarized as: a) during the event the wind-induced offshore current entrains subsurface water in the central gulf, thus establishing the initial density gradient; b) also during the event, the horizontal density gradient is maintained by horizontal warm water advection; c) after the event a coastal jet separates from the west coast reaches the central gulf and spins up to form an anticyclone; d) subduction due to intense convergence occurs where the warm coastal jet meets the cool water; e) the 'mature' warm eddy propagates offshore carrying a lens of cool subducted water within its boundary.

KEY WORDS: Gulf of Tehuantepec, eddy dynamics, subduction, fronts, entrainment.

1. INTRODUCTION

Subduction is defined as the process by which convergence in the mixed layer induces the formerly turbulent fluid to become part of the underlying stratus (Cushman-Roisin, 1987). It is synonymous with ventilation for the continuously stratified ocean and is the opposite of entrainment. Spall (1995) (hereinafter referred to as S95) applies the term to frontal regions and defines it as the process by which water is transferred from the mixed layer into the stratified interior of the ocean.

A frontal region will occur where light and heavy water collide. In an idealized fluid, disregarding for the moment turbulent mixing processes and rotation, a heavy surface water mass colliding with a lighter one would seek its neutral buoyancy level. The balance of the pressure gradient with gravitational and buoyancy forces determines the path.

Any heavy water remaining after the collision will sink below the light side of the front following an isopycnal path. The impermeability theorem (Haynes and McIntyre, 1987) states that isopycnal surfaces are impermeable to changes in potential vorticity (stratification), even in the presence of buoyancy forcing and frictional forces. Marshall and Nurser (1992) apply this result to the ventilated thermocline of a subtropical gyre. They conclude that the flux of potential vorticity (or stratification) between two isopycnal surfaces can emanate only from the free surface or from a solid boundary. This is the case of the surface frontal regions discussed here, only at a smaller scale. We describe the redistribution and mixing of properties along approximately isopycnal trajectories. The process is therefore referred to as isopycnal mixing, to distinguish it from the diapycnal type of mixing (across density surfaces) which is associated with entrainment.

Subduction in mesoscale features does not always take place. In a rotating ocean the flow is compounded by the presence of currents along the front. The shear in these currents could mix and disintegrate the water mass before any vertical motion takes place. Additionally, atmospheric forcing is also capable of mixing that could inhibit subduction. In order for subduction to occur, the flow in the frontal region must have a significant ageostrophic component capable of inducing downward cross-isobaric motion, or else other processes will dominate the dynamics (see, for instance S95 and Hoskins, 1982).

In the Gulf of Tehuantepec (Figure 1), intense surface cooling and dramatic changes in the near-surface coastal circulation are produced every winter by short-lived (3 to 7 days) southward wind events locally known as 'Nortes'. The surface cooling is due to entrainment of subsurface water induced by the vertical shear within a southward current jet produced by the wind (Trasviña *et al.*, 1995). The surface temperature anomaly takes the shape of an elongated patch of water, significantly colder (17 to 22°C) than the surrounding ocean (28 to 30°C). Cool patches of this kind show in the infrared imagery surrounded by intense thermal fronts which extend to a distance of 450 km from shore (Strong *et al.,* 1972; Stumpf, 1975; Stumpf and Legeckis, 1977). Such a large volume could conceivably spin up to

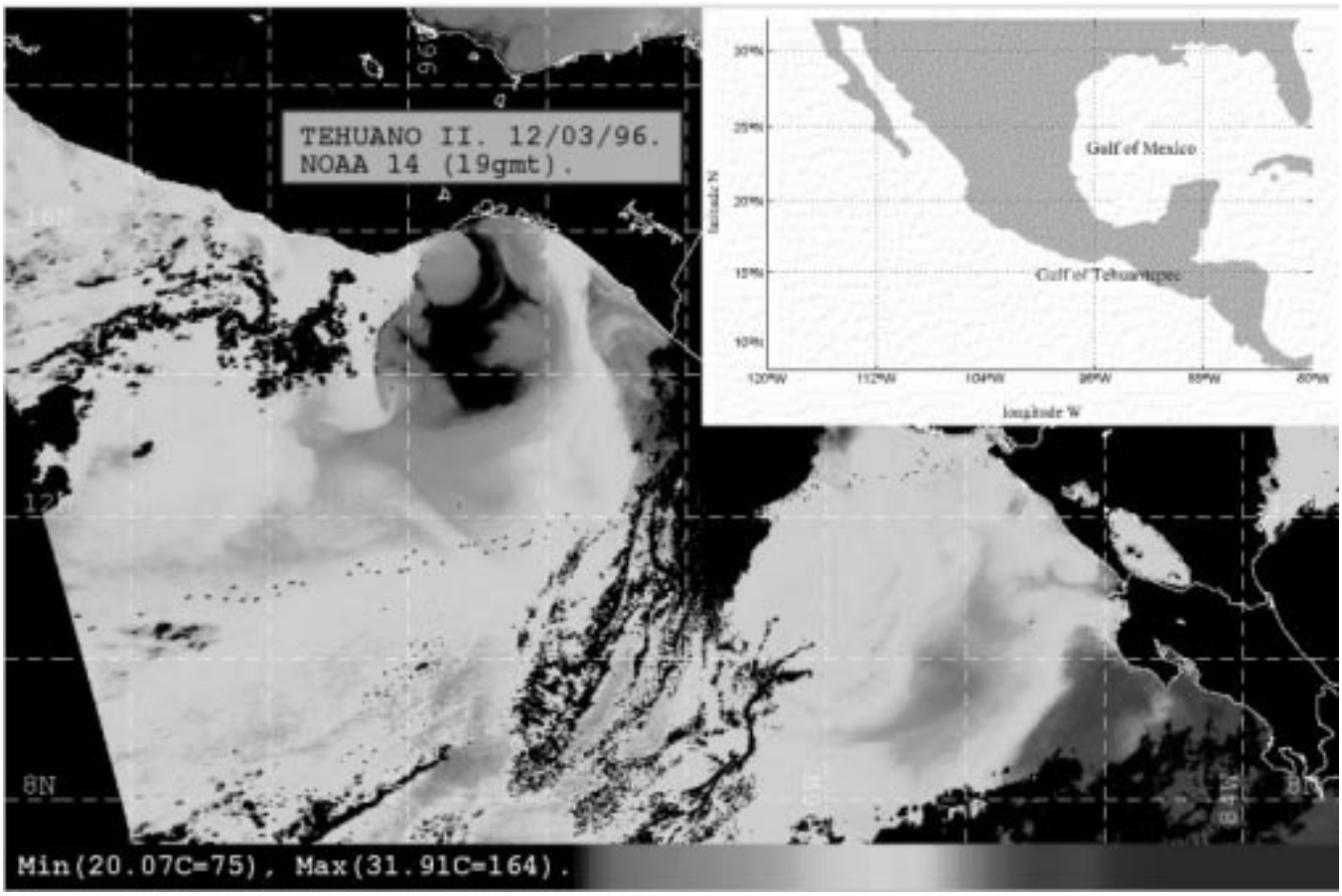

Fig. 1. The Gulf of Tehuantepec: AVHRR image showing surface cooling.

form a cyclonic eddy. Instead, strong warm water advection from both sides of the anomaly make its surface signature disappear in three to four days (*Trasviña et al.,* 1995). Heat fluxes across the air-sea interface are not strong enough to account for the quick change in sea surface temperature (*Barton et al.*, 1993).

Section 2 describes data obtained in two experimental campaigns. Section 3 presents observational evidence of subduction beneath the western temperature front of an eddy. The discussion in section 4 focuses on explaining the phenomenon in terms of vorticity variations. A final section includes a conceptual scheme of the eddy generation process, as well as some remarks on the relevance of the phenomenon.

2. OBSERVATIONAL CAMPAIGNS

2.1. January-February 1989 (Tehuano I)

This campaign was designed to study the impact of Norte wind events in the Gulf of Tehuantepec. During this experiment we carried out conventional CTD (conductivity, temperature, and depth probe) casts, undulating CTD tows (Seasoar), as well as current measurements with a shipboard 150 kHz narrowband ADCP (Acoustic Doppler Current Profiler). AVHRR (Advanced Very High-Resolution Radiometer) satellite imagery was available throughout the experiment. A variety of other instruments were deployed, both moored and on the coast. Barton *et al.* (1993) gives an overview of the observational campaign.

Two research vessels participated in the 40-day campaign but only data from the cruise of R/V Wecoma (Oregon State University) are shown here. This ship gathered hydrographic and meteorological data along an east-west grid, between January 14 and February 9, 1989. Figure 2 shows the transects discussed here.

The Seasoar undulating vehicle for the CTD included a faired cable, which allowed us to tow it at speeds of 8 to 10 knots profiling between the surface and 300 m roughly every 10 min. The typical horizontal resolution of the hydrographic casts is 3 km. The shipboard ADCP was configured to average raw pings every 10 min, in vertical bins of 8 m. The horizontal resolution of the vertical current profiles was equal or better to that of Seasoar.

The CTD used for both conventional and Seasoar profiles was a Neil Brown Mark III B sampling conductivity, temperature and pressure at 32 Hz. The instrument was calibrated before the cruise and post-calibration of the salinity data was made with bench-salinometer measurements of deep (600 m) water samples taken from the rosette.

2.2. February-March 1996 (Tehuano II)

Seven years later, a second experiment was carried out to follow the propagation of eddies formed in the Gulf of Tehuantepec during the Norte season. Surface current data comes from ARGOS drifting buoys deployed in mid-February 1996. Hydrographic data was gathered from the B.O. Fco. de Ulloa (CICESE). We used both conventional CTD casts and undulating CTD tows (UCTDs). The map of the cruise track (see section 3.2, Figure 5b) along 13°N (the only one shown here) includes positions from four ARGOS drifters and the location of the transect relative to the drifter trajectories. Drifter data was gathered by the Data Assembly Center (DAC) at the Global Drifter Center (Atlantic Oceanographic Marine Laboratory, Miami, Florida). ARGOS positions are the 6-hourly post-processed data provided by the DAC.

Conventional CTD casts were made with a full-ocean depth Seabird SBE9/11 sampling temperature, conductivity and pressure at 24 Hz.

UCTDs were carried out by towing a vehicle containing a Seabird SBE19 CTD, following the method described by Filonov *et al*. (1996). The vehicle containing the CTD is equipped with wings in order to keep it near the surface while towed. Vertical profiles are made by circling a particular station with the ship, or by simply stopping the ship. We used the circling method because it kept the ship from drifting. The CTD sinks to a depth depending on the length of cable and stores the measurements in its internal data logger. The SBE19 sampled temperature, conductivity and pressure at 2 Hz. A method to obtain salinity from temperature and conductivity measured at variable profiling speeds is described in Trasviña (1999). The horizontal resolution of the vertical profiles obtained with the undulating CTD is of 3 to 5 km.

Both instruments were calibrated before the cruise and a post-calibration check of the salinity values was made against bench-salinometer measurements of deep (1000 m) water samples taken from the rosette.

3. FRONTAL SUBDUCTION: OBSERVATIONAL EVIDENCE

3.1. January-February 1989 (Tehuano I)

This experiment succeeded in gathering observations during and after a moderately strong southward wind event. The event started early on January 21, wind speeds reaching 17 ms^{-1} for about 12 hours. By the end of January 23 the winds decreased to 9 ms^{-1} and by late January 24 they were

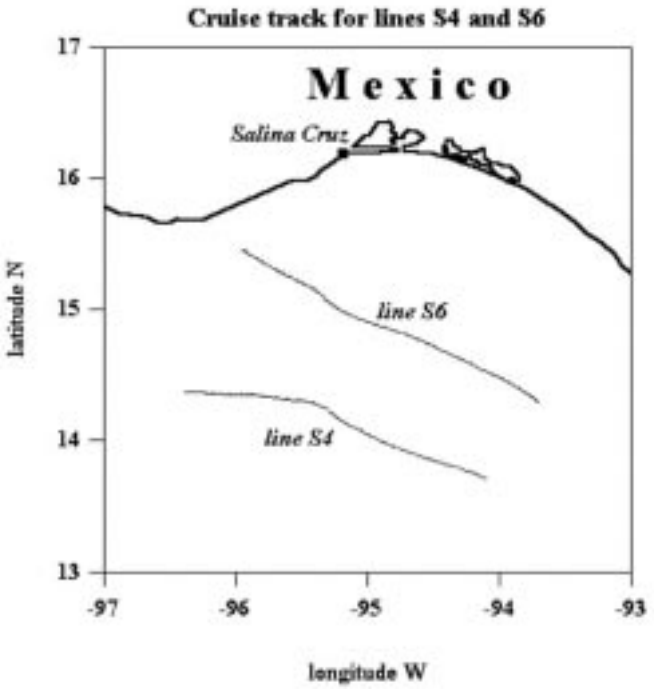

Fig. 2. Transects S4 and S6 carried out during the Tehuano I campaign, January-February, 1989.

completely calm. The whole event lasted almost 3 days. The observations discussed here were gathered after the end of the event, from January 23 to January 25, during a Seasoar-ADCP survey.

The satellite image of January 23 (Figure 3a) shows the response of the upper ocean to the wind event of January 21. The patch of cool water in the central gulf (as defined by the 25°C isotherm) extends from the head of the gulf to almost 300 km offshore. Low sea surface temperatures (SSTs) are still present 450 km offshore within a cool filament extending to the southwest from the southern tip of the patch. Temperatures inside the patch range from 16 to 22°C, with the minimum at about 14.5°N, 95.5°W. Thermal fronts clearly define the shape of the temperature anomaly, the western being considerably stronger than the eastern one. The region of warm water to the west of the temperature minimum (shown in the figure with temperatures between 24 and 25°C) later develops into a 200-km diameter anticyclonic eddy (Trasviña *et al.,* 1995). SSTs outside the patch range between 28 and 30°C. Line S4 of the Seasoar-ADCP survey started on January 23 and traversed the gulf from west to east. Surface currents (20 m) along this leg are superimposed onto the temperature field. The warm water west of the anomaly already shows anticyclonic rotation. The flow reaches the highest speeds (over 1 ms^{-1}) at the temperature front, and is much weaker inside the cool patch (to about 0.5 ms^{-1}). This shows significant lateral shear in the frontal region. Within the cool patch the flow is relatively uniform although a small degree of convergence towards the western front is suggested by its westward component. These features can also be observed in the vertical section (Figure 3c). East of 95°W the flow becomes irregular over the weak eastern front and then shifts sharply in direction towards the coast. On both boundaries of the colder region significant horizontal shear is found, but is stronger to the west.

In the vertical sections (Figures 3b and 3c) the flow is clearly more intense in the upper layer, above the pycnocline. This surface-trapped flow presents highest vertical shear (0.04 s^{-1}) (Trasviña *et al.*, 1995) in the central and eastern gulf, where the pycnocline is closest to the surface. In the central gulf (around 95.75°W in the density section and around 24 d in the ADCP current section) a dramatic weakening of the pycnocline is accompanied by deep penetration of the surface flow. Trasviña *et al.* (1995), based on observed low values of Richardson numbers (< 0.25), show this weakening to result from shear-induced vertical mixing occurring immediately before this line (S3, Figure 3b) was traversed. To both the east and west of this central region the pycnocline is stronger and the vertical coherency of the flow becomes restricted to the upper layer. Lateral shear observed at the surface of the western thermal front decreases with depth and disappears at about 60 m depth. Since the lateral spacing of the observations is 3 orders of magnitude higher than the vertical one, an estimate of lateral shear comparable with those of vertical shear cannot be obtained.

Summarizing, this cool water patch is about 300 km long, 50 km wide (bound by the 25°C isotherm) and some 60 m deep (bound by the 26 kg m^{-3} isopycnal). These length scales are sufficient to generate a cyclonic eddy since the internal Rossby radius varies here between 30 and 50 km. However, the offshore flow inside the patch was produced by wind forcing less than one inertial period prior to these observations ($T_i=2\pi/f$=46 h at latitude 15°) and, clearly, it has not reached geostrophic balance. In addition, lateral shear across the western thermal front promotes mixing with warmer waters to the west. This surface water mass is therefore transitory. Mixing with warm water quickly reduces its surface signature. A more permanent feature is found below the surface, as shown next.

On January 24 (Figure 4a) the size of the cool patch is greatly reduced. The area traversed the previous day (line S4) still shows minimum SSTs but now they only reach about 20°C. Seasoar-ADCP line S6 was traversed on 24-25 January. It runs closer to shore than line S4 and traverses an area that was occupied by low SSTs the previous day (see also Figure 3a). At the time of the crossing intense currents from the west (about 1 ms^{-1}) cover the surface with warm waters (over 25°C). Only to the north of line S6, in the cen-

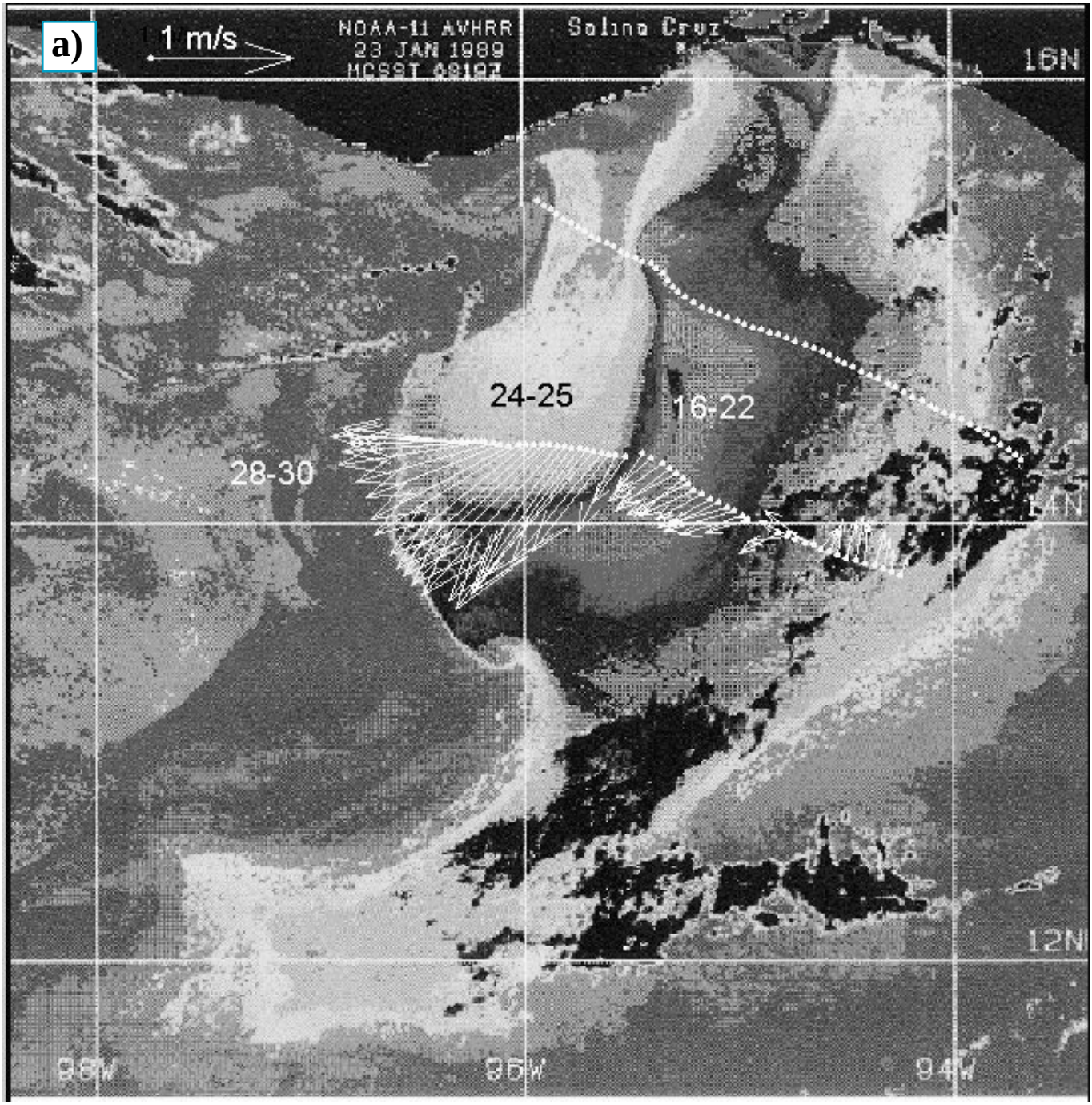

Fig. 3. a) Satellite image of 23 January, 1989. Superimposed are surface velocity vectors from ADCP (line S4). Note the temperature ranges for different gray values. The track for next day's line S6 is included as reference (see text); b). Density anomaly (γ) section along line S4; c) Stick diagram of surface flow from ADCP.

tral gulf, a curved filament of cool water remains (starting at about 15°N 95.2°W). Surface currents around the front reveal intense convergence and lateral shear. The front separates two distinct current regimes. In the west the currents rotate in anticyclonic sense in a somewhat asymmetric way providing the flow with a significant eastward component. In the central gulf the offshore flow observed the previous day, even if slightly weaker, remains the dominant feature.

In the density section along S6 (Figure 4b), a steep front appears at the region of convergence of the surface flow (between 95.5 and 95°W). West of 95.2°W the pycnocline takes

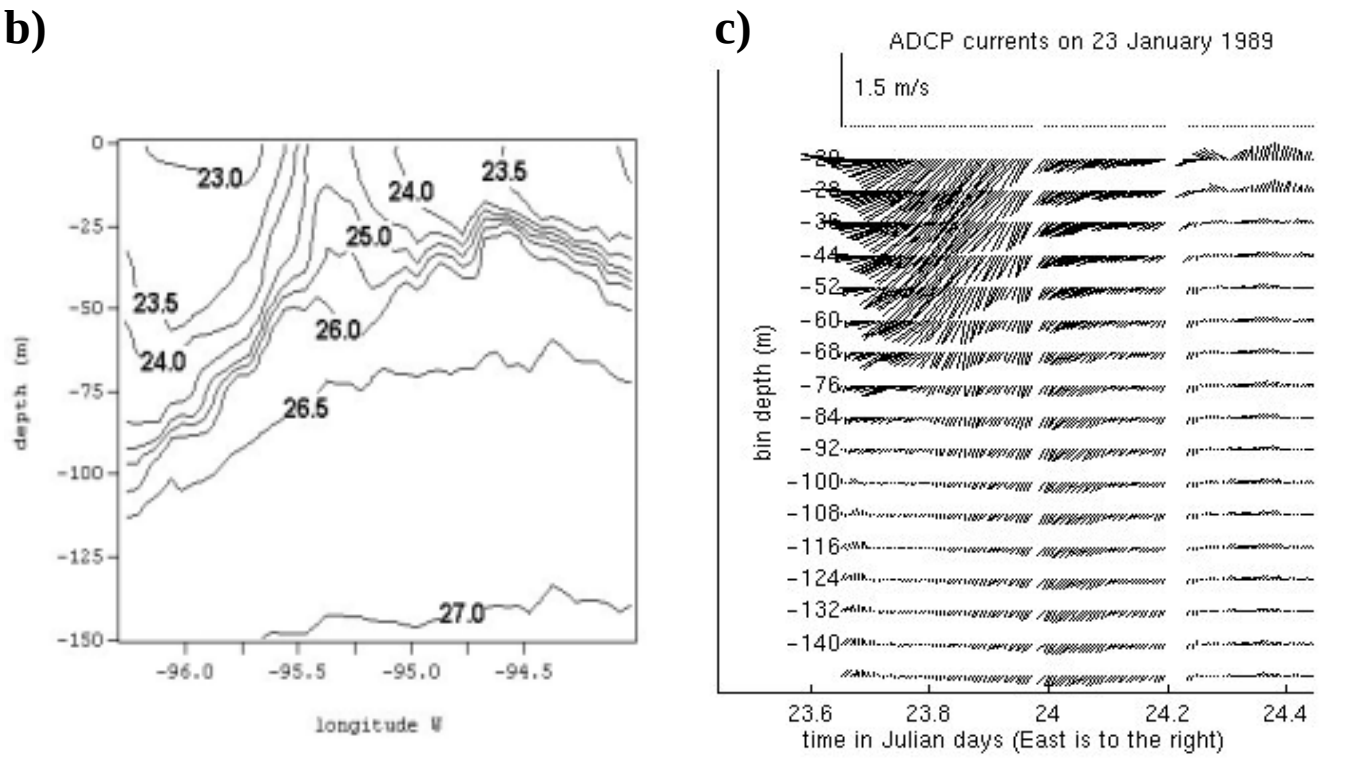

Fig. 3. Continued.

the typical concave shape associated with anticyclonic eddies. Within this pycnocline a 'lens' with density anomalies (γ) between 25 and 26.5 kg m^{-3} is apparent (its core is highlighted with gray dots). This density range corresponds to those observed the previous day at or near the surface of the central gulf (see also Figure 3b), about 40 km north of line S6. Note also that on January 23 (Figure 3a) the cool patch extended to the area traversed by S6 the next day. The presence of this lens is consistent with the subduction of the anomalously cold (and heavy) surface water mass produced by the wind event. The current regime (Figure 4c) supports this assumption. Around the density front the flow shows intense convergence reaching depths of 80 m around the area of the lens. As observed in the previous crossing (Figure 3c), the currents are more intense above the pycnocline but now the maximum vertical penetration occurs at the density front, where the pycnocline deepens dramatically.

Summarizing, the crossing of line S6 reveals a lens of water within the pycnocline. The density range within it (γ= 24 to 25.5), as well as its temperatures and salinities (not shown), closely correspond to those found the previous day at the surface of the cool patch. The flow field converges around the front, from the surface to 80 m depth. Since no measurements were made along line S6 the previous day, some conditions before subduction remain unknown. For instance, it is not known if the mixed layer was deeper or shallower than the front before subduction took place. However the observational evidence is consistent with intense subduction taking place within the 24 hours prior to this crossing. The presence of a dense surface water mass on 23 January and the location of a lens at an average depth pf 80 m, 24 hours later, suggests a subduction rate as high as 80 m d^{-1}. This is comparable to what was reported by Flament *et al.* (1985) in a similar frontal structure of an upwelling filament. Before discussing the dynamics, the next section describes similar observations inside an eddy found off Tehuantepec in 1996.

3.2. February-March 1996 (Tehuano II)

During this campaign a number of ARGOS drifters were deployed inside a large anticyclone formed in the gulf of Tehuantepec before February 10, 1996. The anticyclone originated during a wind event that occurred the week prior to drifter deployment. No data from that wind event are available.

Drifter deployment started on February 10 with the arrival of the first ship to the area. The initial effort was concentrated on an eddy that had a clear thermal signature in the AVHRR imagery (Figure 5a). Between February 10 and 11, four drifters were deployed in its interior and tracked till March 7 (Figure 5b). Undulating CTD tows were made between February 23 and 26 along line about 13°N (track shown on Figure 5b).

In the image of February 11 (Figure 5a) surface temperatures at the core of the eddy are greater than 28°C. East of 96°W the cool surface waters are produced by a wind event that started the morning of that day. Close to the coast (15°N, 96°W) the warm feature intruding the cool waters east of 96°W represents another eddy in formation. This was later 'seeded' with drifters and its circulation followed for several months (tracks not shown).

Positions from four surface drifters are shown in Figure 5b. They follow the slow south-westward motion of the eddy between February 11 and March 7. The CTD section along 13°N traversed the area some 12 days after drifter deployment (also shown in Figure 5b). It crosses the southern half of the anticyclone, some 50 km south of the center of motion.

The vertical density section along 13°N (Figure 5c) was obtained between February 23 and 26 and it features the concave pycnocline typical of warm eddies, reaching some 200 m depth. Its horizontal span is surprisingly large. The eddy seen in the imagery and in the drifter tracks occupies less than 3 degrees (some 300 km) in the zonal direction but, if the shape of the pycnocline is used as reference, the eddy spans at least 4 degrees of longitude. This is attributed to the reduction of its surface thermal signature by the invasion of cool surface water produced by the wind event of February 11. The eastern half of the eddy again shows a lens in the pycnocline (highlighted with gray dots between γ=24 and 26.5). This is better developed than the one observed in 1989. It occupies a larger fraction of the volume of the eddy and it is not, as in the previous case, sloping along the eastern border. Instead, it is found closer to the bottom of the eddy. The lens in the 1989 eddy only spanned some 40 to 50 m of the water column whereas this one covers 80 to 100 m. The 1989 eddy was 3 days old and this one is over 13 days old.

A second occurrence of an intrapycnocline lens in a Tehuantepec eddy suggests that they are related to the eddy generating process. It also reveals that these are stable features since this lens was observed at least 13 days after the birth of the eddy. In this case the eddy (and the lens) has had more than enough time to reach geostrophic balance. Furthermore, the large volume of the lens in 1996 suggests it may exert significant influence on the internal eddy dynamics. Such an asymmetric stratification field will produce an asymmetric tri-dimensional vorticity distribution within the eddy. Orbital speeds will vary and therefore its propagation velocity should be altered. Drifter tracks appear to confirm this observation. The eddy describes an unusual southwestward propagation (in contrast with westward self-propagation, see Figure 10), conceivably produced by this feature although a detailed analysis of the eddy dynamics are deferred to another paper.

4. DISCUSSION

Data from the Tehuano I experiment captured the early stages of both an eddy and its accompanying lens. To better understand the origin of such a lens it is helpful to analyze the behavior of a conservative property. Salinity serves such a purpose for the time scales (< 2 d) considered here. The structure of the central gulf immediately after a wind event is shown with isobaric and isopycnal sections of line S4 (Figure 6). The isobaric section (Figure 6a) is very similar in structure to the corresponding density section (Figure 3b). High salinity values reach the surface of the central gulf (95.25°W). As previously mentioned, this results from entrainment of subsurface water. Two fronts border this central region. The eastern one is weak and shallow, and the western front is stronger and deepens to 100 m with a steep slope. The latter is the eastern boundary of an eddy in its early stages of development. Note the curvature of the isohaline of 34.4 for future reference and the boundaries of the surface high-salinity region of the central gulf (34.5 to 34.8).

In the isopycnal salinity section (Figure 6b) the fronts and, in general, the halocline are expanded revealing different response patterns across the gulf. In the central and eastern side (east of 95.25°W) the isohalines follow the complex behavior typical of dyapicnal mixing. In the western gulf, although the isobaric section shows deepening of the vertical structure, little mixing across density surfaces takes place. Defining the core of the eddy as bounded by the 34.4 isohaline, its alignment with the density field is consistent with mixing processes (and water mass generation) along density surfaces.

The comparison between the isobaric and isopycnal sections of line S6 (Figure 7) traversed the following day is even more dramatic. In the isobaric section (Figure 7a) a high-salinity lens of the same salinity range found at the surface of S4 (34.8 to 34.5 psu), is now found deep within the halocline of the eddy. An even steeper salinity front appears at the boundary between the eddy and the offshore flow of the central gulf. Because of intense advection from the west (see also Figure 4c), the front is found eastward of its position on S4. It is now centered at about 95°W. The central and eastern gulf (now east of 94.8°W) show a mostly flat halocline. Also, as observed in the density section (Figure 4b), the stratification of the upper 50 m of the eastern gulf is greater than in the previous crossing.

The isopycnal section (Figure 7b) presents a situation similar to the one observed the previous day. To the west of 94.8°W there is little dyapicnal mixing whereas in the east mixing across density surfaces occurs even against strong stratification (not shown). The region of the intra-pycnocline

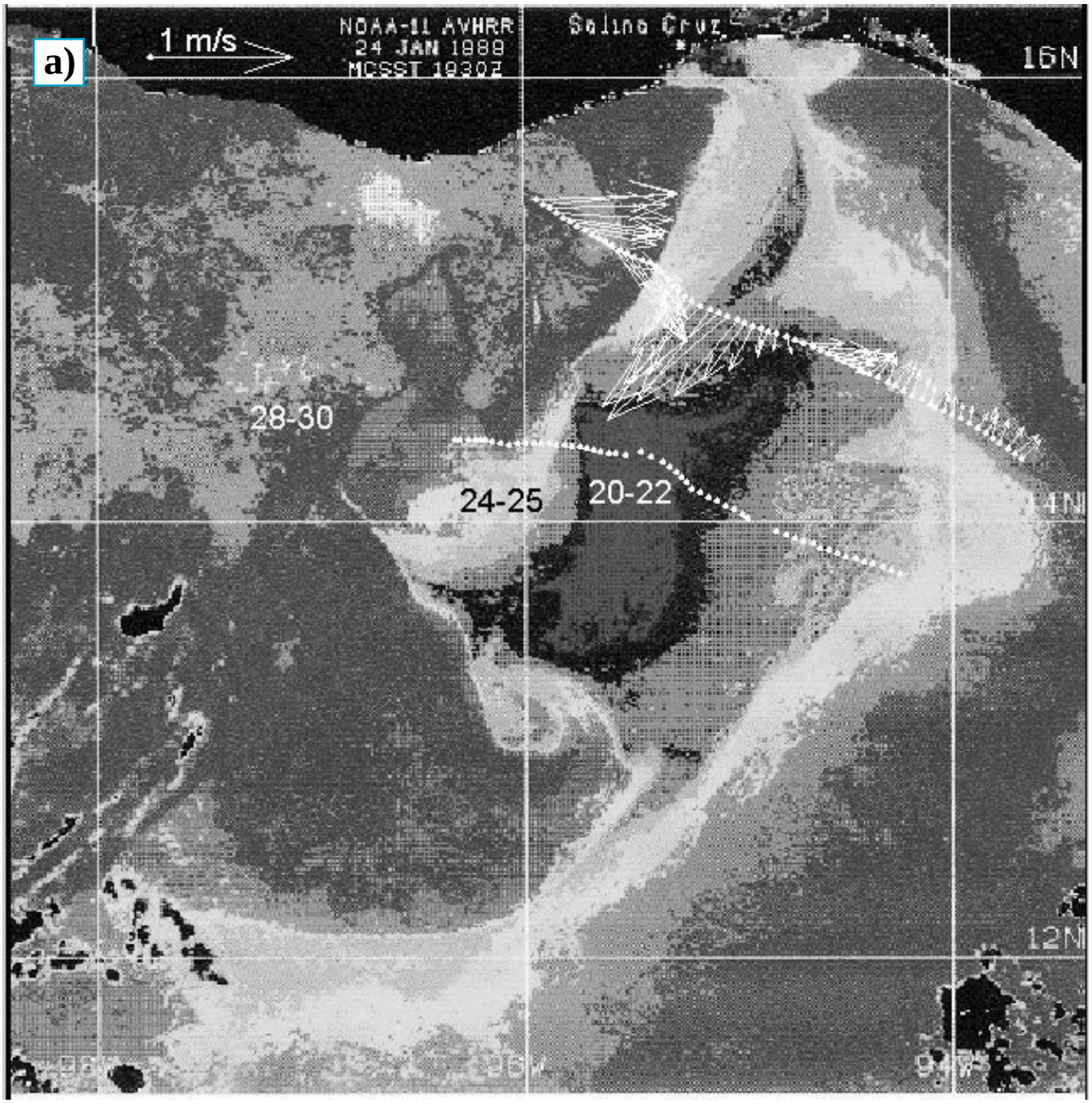

Fig. 4. a) Satellite image of 24 January, 1989. Superimposed are surface velocity vectors from ADCP (line S6). Note the temperature ranges for different gray values. The track for line S4 is included as reference (see text); b) Density anomaly (γ) section along line S6 ('lens' highlighted with gray dots); c) Stick diagram of surface flow from ADCP.

(or, in this case, intra-halocline) lens is now found west of 95°W and between γ=24 and 26.5. Compared to the complex patterns of the salinity field east of 95°W, in this region it is remarkably well aligned with the density surfaces, consistent with the existence of isopycnal mixing. This term is used to emphasize that water masses of different origins will have different compositions (nutrients, dissolved oxygen, chlorophyll, etc.) at equivalent density ranges. When motion along a density surface takes place, mixing of a number of properties is bound to occur (McDougall, 1984). It also helps in differentiating from the dyapicnal processes, which dominate in the rest of the gulf. Dyapicnal mixing is associated to vertical shear-induced entrainment in regions of the gulf influenced by intense surface currents. Isopycnal mixing is

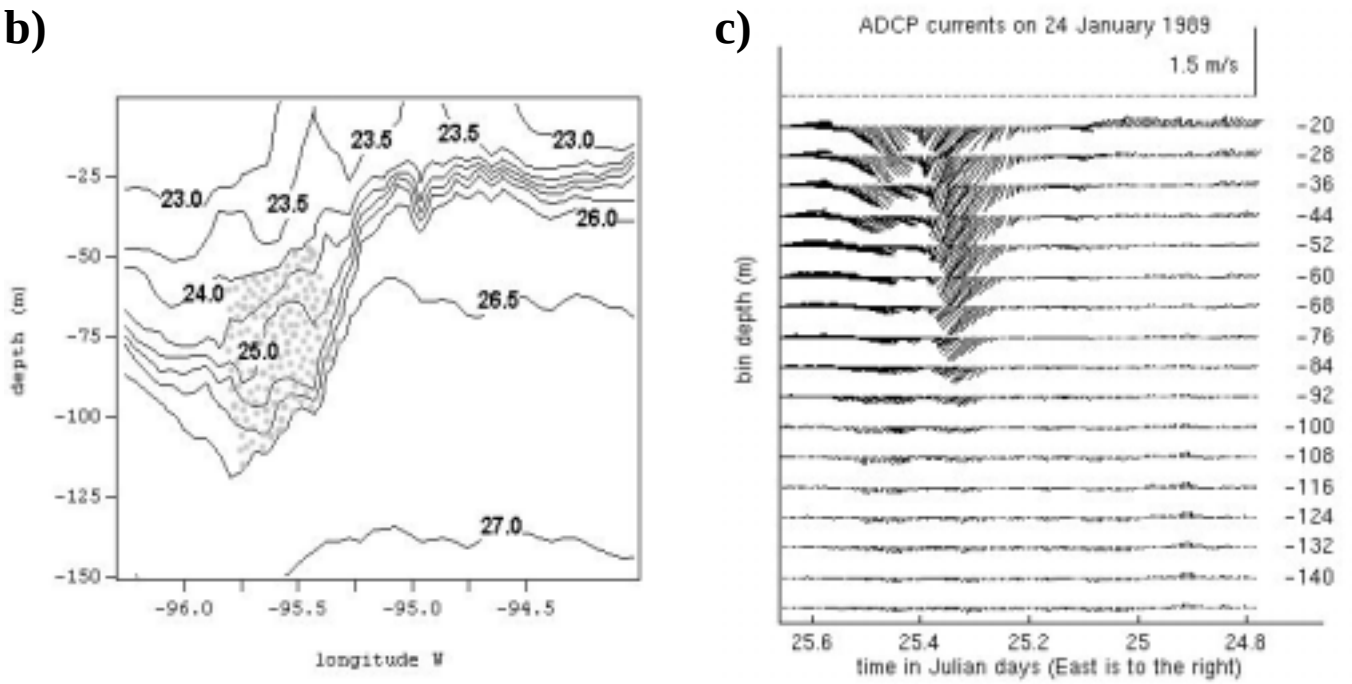

Fig. 4. Continued.

found mainly along the frontal region where the eastward flow converges with the southwestward (offshore) wind-induced flow. The frontal region separates two different dynamics with contrasting stratification and, consequently, potential vorticity.

Until now flow convergence (and downwelling speed) is suggested by the observations but no quantitative proof has been given. Given the strong time-dependency of the flow, reliable estimates of convergence by means of the mass conservation equation could only be obtained in the along-track direction of this section. The offshore confluence term cannot be accurately estimated. However, it is important to show that there is an ageostrophic downwelling speed capable of producing subduction. Since frontal subduction occurs on a potential vorticity (stratification) gradient, we choose vorticity as a more robust quantity to analyze the nature of the flow. Again, relative vorticity can only be estimated from ($\delta_x v^*$), the along-track derivative of the across-track velocity component (x is positive towards the east, along the track, and v^* is rotated perpendicular to the track, positive towards the north) but it can be checked for consistency with the density field. In any case the assumption is made that ($\delta_y u^*$), the across-track derivative of the along-track velocity component, is negligible (y is positive towards the north, perpendicular to the track; u^* is rotated to be positive to the east, along the track). This is not true in general, but for scales of the order of the internal Rossby radius (30 to 50 km) an inspection of the density and current fields supports this assumption.

The average relative vorticity (ξ) was calculated between isopycnal surfaces limiting the lens (γ = 24 and 25.5 kg m^{-3}, see also Figure 4b). Figure 8a shows relative vorticity along line S6 as the non-dimensional parameter (ξ/f), f being the local Coriolis parameter. This also serves as an estimate of the Rossby number of the flow. Potential vorticity (Figure 8b) was calculated as $\Pi = (\xi + f)/H$, where H is the thickness between density surfaces 24 and 25.5 kg m^{-3}.

The relative vorticity (Figure 8a) is small and featureless throughout the section except by the steep gradient found at the density front. Large positive values at the central gulf (95°W) are comparable with those of the planetary vorticity. This indicates that advective processes are still important in the offshore current jet. Within the lens (95.4 to 95.1°W) the relative vorticity changes sign reaching a minimum consistent with the induction of anticyclonic rotation by vortex compression. The potential vorticity (Figure 8b) also shows a steep gradient at the central gulf. Π serves to compare changes in absolute vorticity (ξ+f) with those of layer thickness (H). At the central gulf the combined effect of an increase in stratification (a decrease in layer thickness) and intense advection leads to the central maximum. To the east any changes in Π are produced mostly by changes in layer thickness since the relative vorticity is almost negligible. In the west the small values of Π are due to the increased layer thickness within the lens and to the small values of the absolute vorticity.

Evidence from two independent variables, the observed flow and the density field, confirm the existence of subduc-

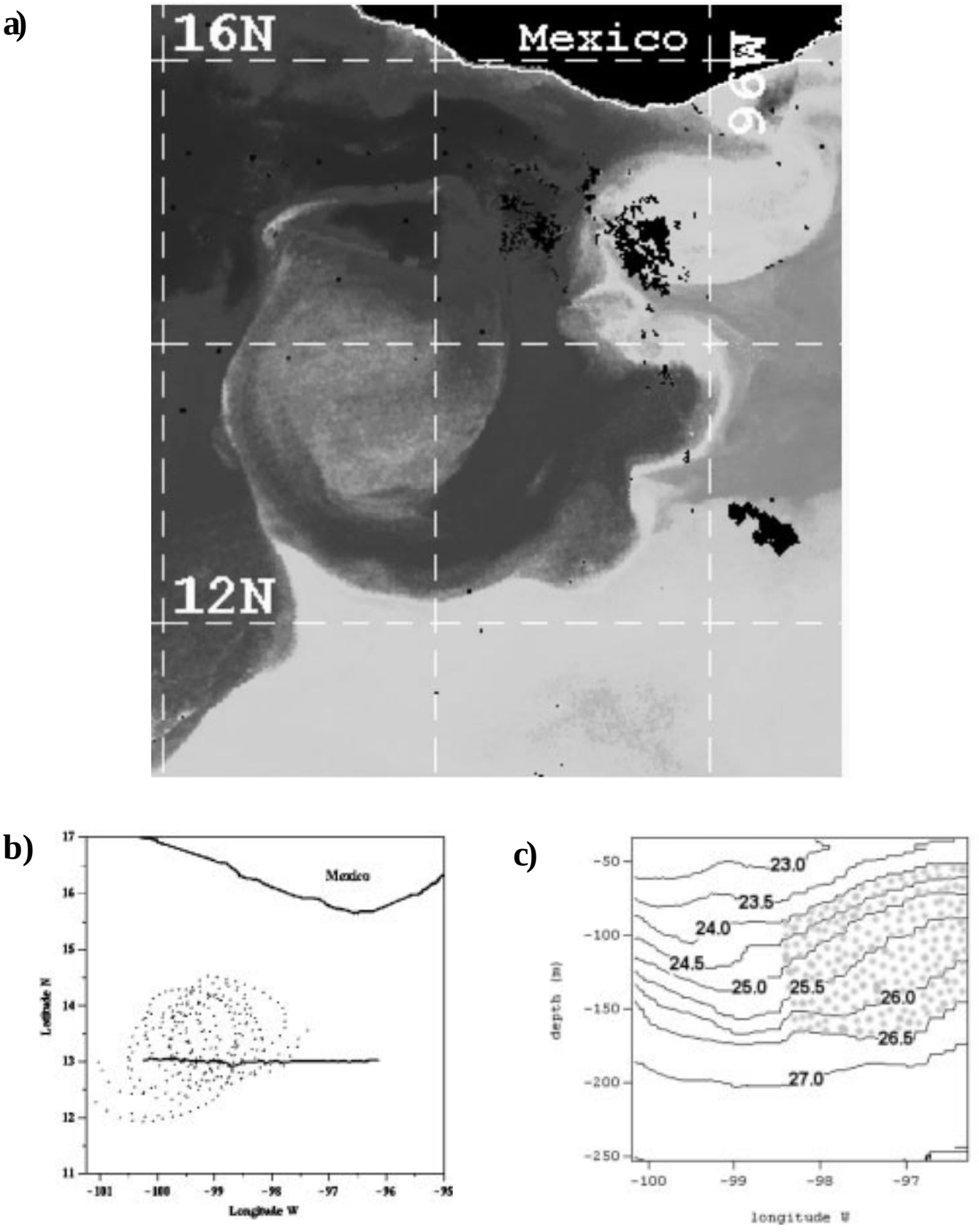

Fig. 5. a) AVHRR image of Eddy 1 on February 11, 1996; b) Drifter tracks inside Eddy 1 (February 11 to 7 March, 1996) and track along 13°N (solid line); c) Density anomaly (γ) section along 13°N. The line was traversed between February 23 and 26, 1996.

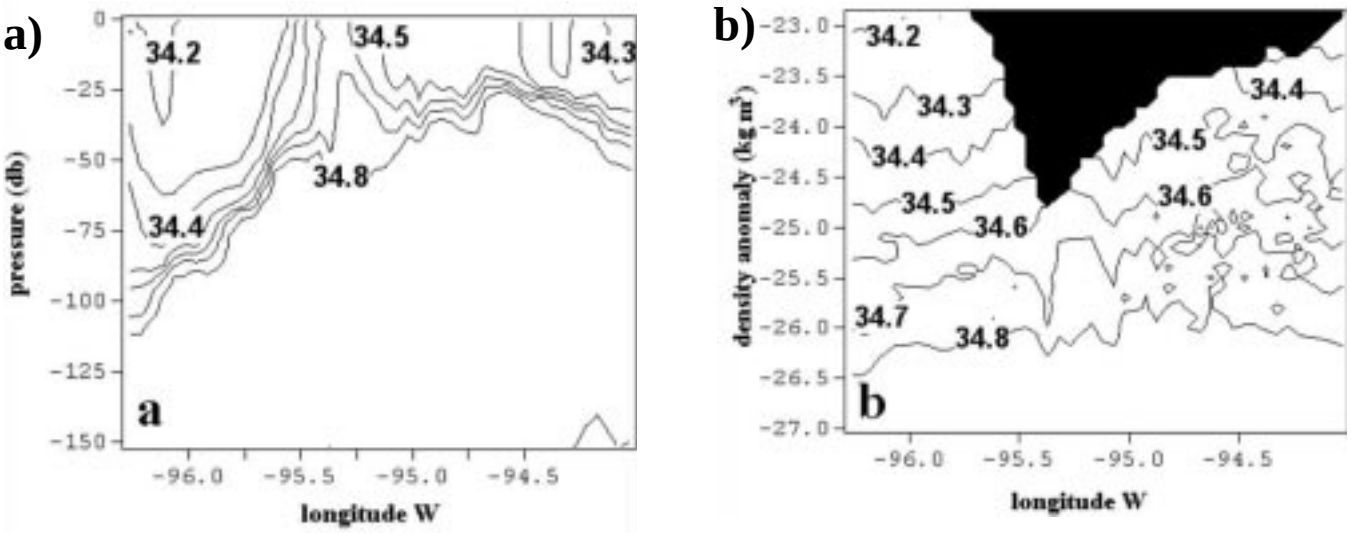

Fig. 6. a) Isobaric salinity section along line S4, 23-24 January, 1989; b) Isopycnic salinity section along line S4.

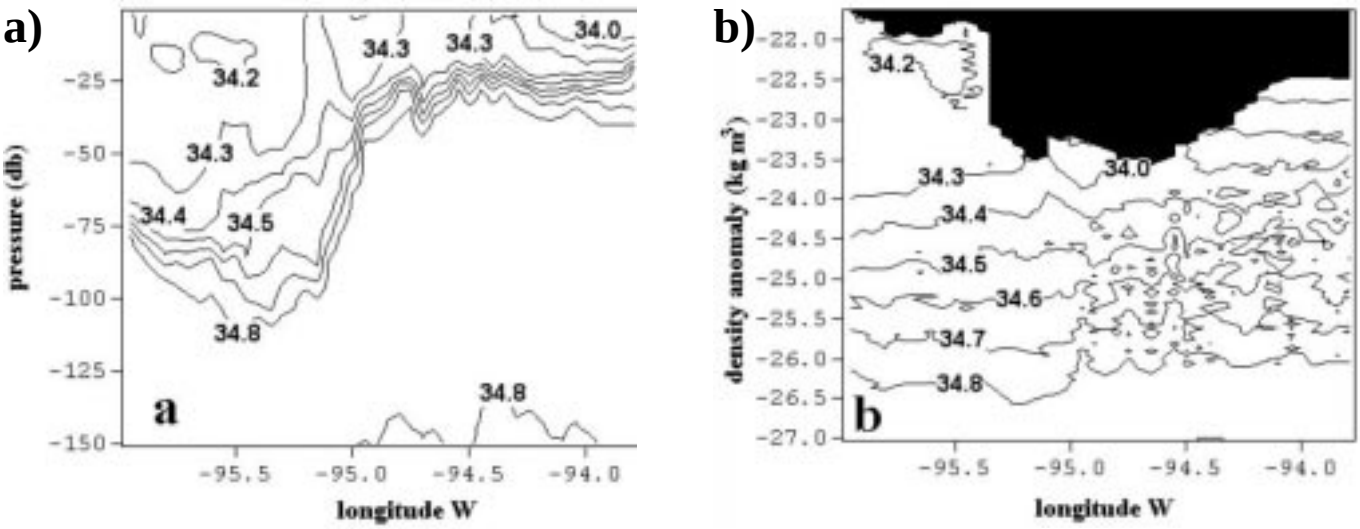

Fig. 7. a) Isobaric salinity section along line S6, 24-25 January, 1989; b) Isopycnic salinity section along line S6.

tion processes. The negative relative vorticity minimum is found at the lens. This can only be accomplished by vortex compression. Furthermore, the compression of vortex tubes necessary to produce such a potential vorticity gradient has to be accompanied by downwelling speeds (see, for instance: S95 and Pollard and Regier, 1990).

Finally, ageostrophic velocities (v_a) were estimated from the observed and geostrophic velocity fields (Figure 9). The ADCP currents (observed field) were first rotated relative to the track such that the *v-component* is directed across the track of line S6, positive towards the north (v^*_{obs}). Then v_a was obtained by simply subtracting the geostrophic from the observed field (v^*_{obs}-v_{geo}). Isopycnals are superimposed onto the velocity field. Values smaller than abs (0.2 m s^{-1}) are blanked out to eliminate badly sampled small-scale variability. The ageostrophic component of the flow is negligible except in isolated areas. The positive near-surface maximum east of 95°W occurs within the offshore current jet, in the same area where the local Rossby number reaches a maximum (ξ/f). Two areas of opposite sense inside the lens of subducted water show its anticyclonic nature: offshore ageostrophic flow (~0.5 m s^{-1}) east of 95.25°W and onshore to the west (~0.5 m s^{-1}). Evidence of ageostrophic anticyclonic circulation within the lens clearly shows that it was produced by vortex compression (S95). It also shows that the lens formation process is recent since it hasn't had the time to adjust to geostrophy. The subduction rate of 80

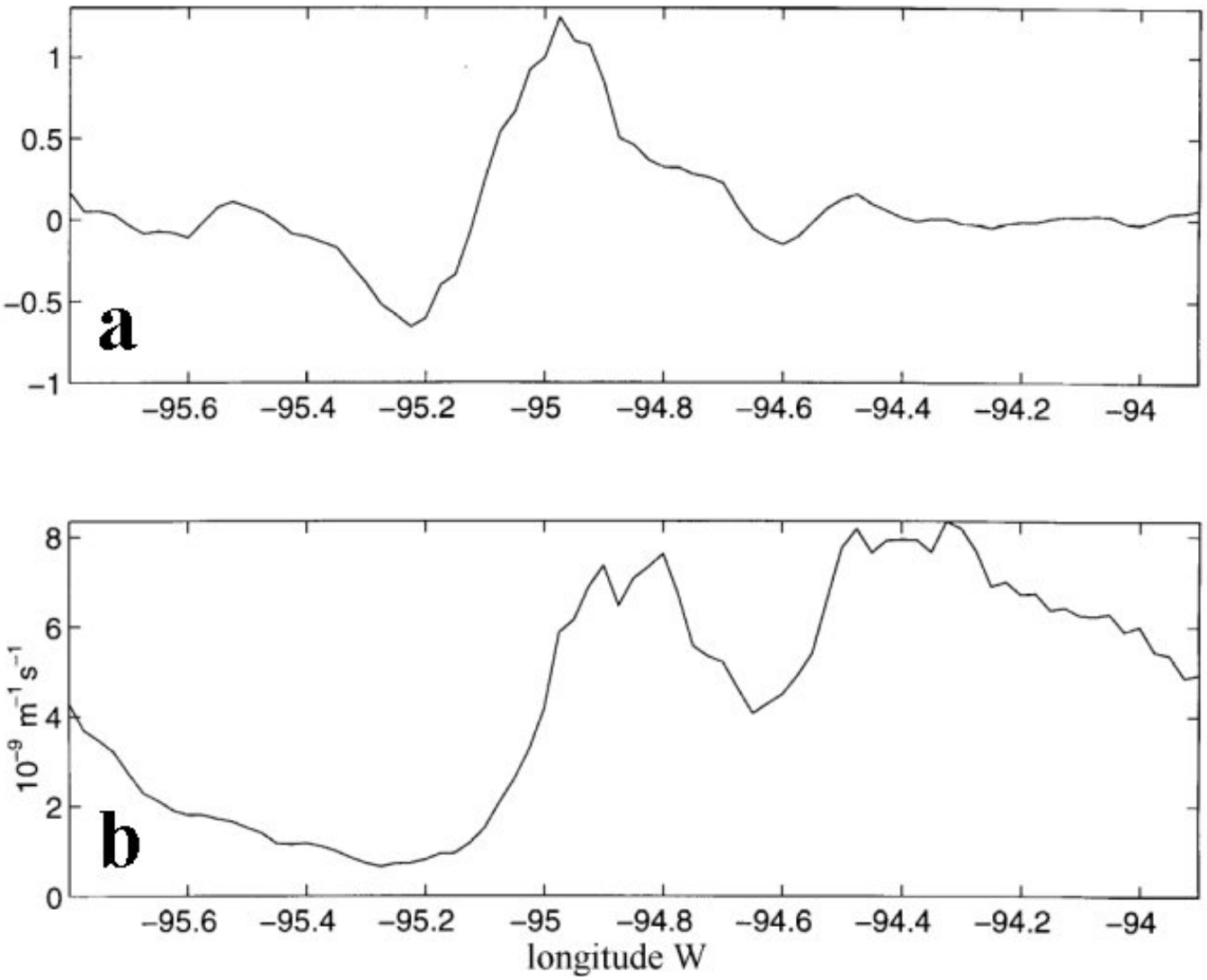

Fig. 8. a) Average relative vorticity (x/*f*) within the intrathermocline lens (between g=24 and 25.5); b) Average potential vorticity (P) for the same isopycnal range as before.

md^{-1} previously mentioned seems now more likely. The conditions leading to the initial subduction are unknown but the production of an anticyclonic lens, as shown by S95, are consistent with a shallow and warm surface flow colliding with a thicker cool surface patch.

5. CONCLUSIONS

The origin of the lens in the 1989 Tehuantepec eddy by subduction is supported by previous modeling work from S95. Spall´s results for frontal subduction with a deep surface layer are characterized by the production of a lens with anomalously low potential vorticity and anticyclonic circulation, same as observed here. There are no observations of the frontal structure to confirm that the mixed layer prior to subduction was actually thicker than the front. However, the presence of a lens of these characteristics is consistent with subduction starting from such an initial condition.

In the Gulf of Tehuantepec, Nortes, and the wind-induced circulation occur regularly during the cold season (September to April). Although there is a great deal of interannual variability (from 0 to 27 Norte-inducing cold surges in a 60-year record), the average is around 13 events per cold season (Schultz *et al.*, 1998). Every time, this phenomenon produces cool surface patches and eddies that may differ in size but that are dynamically very similar. The finding of two occurrences of intrapycnocline lenses is no coincidence. It reveals an interesting feature probably common to many such mesoscale features: eddies within Tehuantepec

eddies. Although the mean ambient flow in this area is not well known, tracks from other drifters deployed by the authors show extremely weak currents outside the mesoscale eddy field. Without the influence of a strong ambient flow, the unusual southwestward propagation of these eddies (see Figure 10) can be attributed to their internal dynamics.

From a previous article (Trasviña *et al.,* 1995) a conceptual model of eddy generation in the Gulf of Tehuantepec could be summarized in three steps:

a) The wind induces an intense offshore current. Vertical shear within the jet produces entrainment of cool subsurface waters. The initial density gradient is established.

b) Still during the wind event, the horizontal density gradient is maintained by advection of light (warm) water from the west. Advection from the east is negligible at this stage.

c) After the end of the wind event, a narrow (and warm) coastal jet separates from the west coast of the gulf. While reaching the central gulf, and the cool patch, it spins up to form the anticyclonic eddy.

Two additional steps can now be added:

d) Where the coastal jet meets the cool water patch, subduction starts due to intense convergence between water masses of contrasting density. Presumably, the depth of the coastal jet is shallower than that of the cool patch and therefore an anticyclonic lens is formed.

e) The 'mature' eddy propagates offshore carrying away coastal (warm) waters and a lens of cooler water as 'memory' of the wind event (Figure 10).

ACKNOWLEDGEMENTS

Funding for this project was provided by the National Council for Science and Technology (Mexico, grants 32500T and 4971-T9406), the Natural Environmental Research Council (United Kingdom, grant GR3/6719), the Division of Oceanology of CICESE and CICESE's campus at Baja California Sur. The Global Drifter Center (NOAA-AOML) was a collaborator in this project within the framework of the Global Drifter Program, they financed the cost of tracking the lagrangian drifters. We thank Peter Niiler for providing the lagrangian drifters used during the 1996 field work. Dave Schultz provided important weather forecasts during the field experiment in 1996. The Coastal Oceanography Laboratory of the Costa Rica National University supplied valuable satellite imagery for the 1996 experiment. Curt Collins made a thorough and very helpful review of the manuscript. We greatly appreciate the hard work of students, technicians, researchers and crew on board the B.O. Fco. De Ulloa (CICESE), B.O. Altair (Armada de México), R/V Wecoma (OSU) and B.O. El Puma (UNAM).

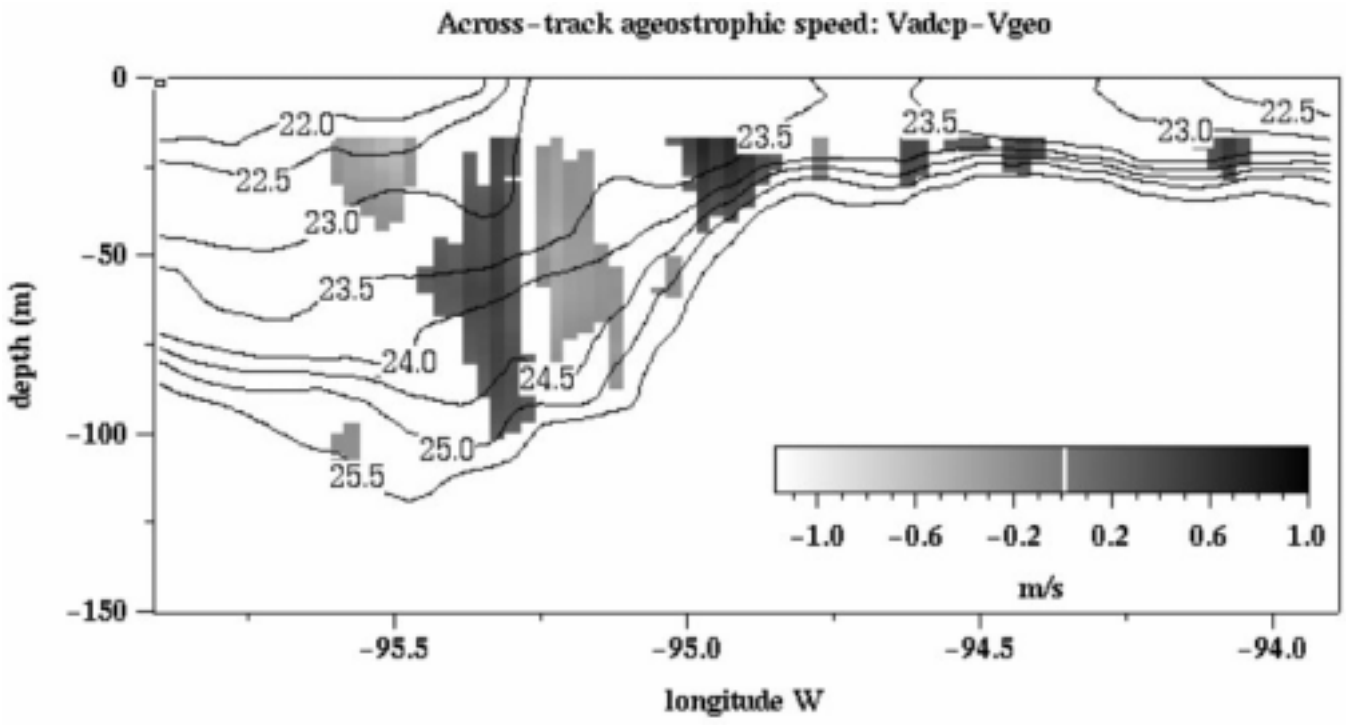

Fig. 9. Across-track ageostrophic speeds along line S6.

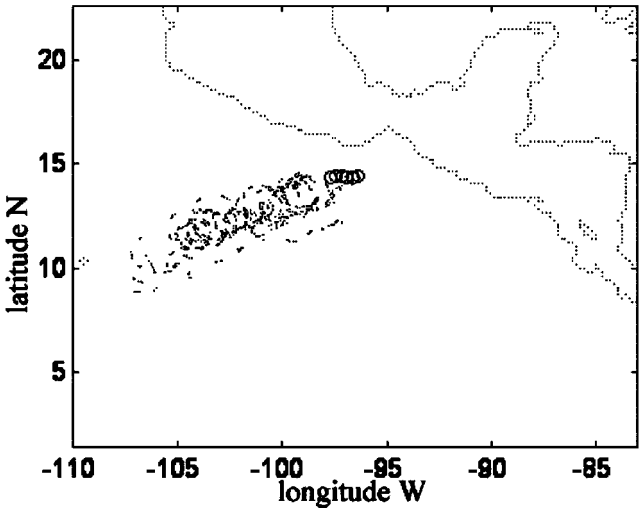

Fig. 10. Southwestward propagation of a Tehuantepec Eddy. Three months of data from ARGOS drifters. Circles indicate deployment sites.

BIBLIOGRAPHY

BARTON, E. D., M. L. ARGOTE, J. BROWN, P. M. KOSRO, M. LAVIN, J. M. ROBLES, R. L. SMITH, A. TRASVIÑA and H. S. VÉLEZ, 1993. Supersquirt: Dynamics of the Gulf of Tehuantepec, Mexico. *Oceanography*, *6,* 1, 23-30.

BLACKBURN, M., 1962. An oceanographic study of the Gulf of Tehuantepec. Spec. Sci. Rep. 404, U.S. Fish and Wildlife Serv., Washington, D. C.

FILONOV, A. E., C. O. MONZÓN and I. E. TERESHCHENKO, 1996. A technique for fast conductivity temperature-depth oceanographic surveys. *Geofís. Int., 35, 4,* 415-420.

FLAMENT, P., L. ARMY and L. WASHBURN, 1985. The evolving structure of an upwelling filament. *J. Geophys. Res., 90(C60)*, 11,765-778.

HAYNES, P. H. and M. E. McIINTYRE, 1987. On the evolution of vorticity and potential vorticity in the presence of diabatic heating and frictional or other forces. *J. Atmos. Sci.*, *44,* 828-841.

MARSHALL, J. C. and A. J. NURSER, 1992. Fluid Dynamics of Oceanic Thermocline Ventilation. *J. Phys. Ocean.*, *22,* 583-595.

McDOUGALL, T. J., 1984. The Relative Roles of Diapycnal and Isopycnal Mixing on Subsurface Water Mass Conversion. *J. Phys. Oceanogr*., *14,* 1577-1589.

POLLARD, R. T. and L. REGIER, 1990. Large variations in potential vorticity at small spatial scales in the upper ocean. *Nature, 348,* 227-229.

SCHULTZ, D. M., E. R. BRACKEN and L. F. BOSART, 1998. Planetary- and Synoptic-Scale Signatures Associated with Central American Cold Surges. *Monthly Weath. Rev.*, *126,* 5-27.

SPALL, M. A., 1995. Frontogenesis, subduction, and cross-front exchange at upper ocean fronts. *J. Geophys. Res.*, *100 (C2), 2,* 543-2,557.

STRONG, A. E., R. J. DE RYCKE and H. G. STUMPF, 1972. Satellite detection of upwelling and cold water eddies, paper presented at 8th International Symposium on Remote Sensing of the Environment. Environ. Res. Inst. of Mich., Ann Arbor, 1067-1081.

STUMPF, H. G., 1975. Satellite detection of upwelling in the Gulf of Tehuantepec, Mexico. *J. Phys. Oceanogr*., *5,* 383-388.

STUMPF, H. G. and R. V. LEGECKIS, 1977. Satellite observations of mesoscale eddy dynamics in the eastern tropical Pacific Ocean. *J. Phys. Oceanogr.*, *7,* 648-658.

TRASVIÑA, A., E. D. BARTON, J. BROWN, H. S. VÉLEZ, M. KOSRO and R. L. SMITH, 1995. Offshore Wind Forcing in the Gulf of Tehuantepec, Mexico: the asymmetric circulation. *J. Geophys. Res.*, *100(C10), 20,* 649-20,663.

TRASVIÑA, A., 1999. Procesamiento de datos de CTD ondulante. *GEOS*, Unión Geofísica Mexicana, 19, 1, 1-11.

A. Trasviña[1], E. D. Barton[2], H. S. Vélez[3] and J. Brown[4]

[1] CICESE, Oceanografía Física, Miraflores 334 e/Mulegé y La Paz, Fracc. Bella Vista, 23050, La Paz BCS, Mexico.
Email: trasvi@cicese.mx
[2] University of Wales, School of Ocean Sciences, Menai Bridge, United Kingdom.
[3] Depto. de Ingeniería y Procesos Hidráulicos. División de Ciencias Básicas e Ingeniería. Universidad Autónoma Metropolitana. Unidad Iztapalapa. México, D.F., México.
[4] Fisheries Laboratories, MAFF, Suffolk, United Kingdom.